Stanford Exploration Project, Report 124, April 4, 2006, pages 1–16

Plane-wave migration in tilted coordinates

Guojian Shan and Biondo Biondi

ABSTRACT

Plane-wave migration in tilted coordinates is powerful to image steeply dipping reflectors, although the one-way wave-equation operator is used. In plane-wave migration, the recorded surface data are transferred to plane-wave data by slant-stack processing. Both the source plane-wave and the corresponding slant-stacking data are extrapolated into the subsurface, and images are generated by cross-correlating these two wavefields. For each plane-wave source, we assign tilted coordinates whose direction depends on the propagation direction of the plane-wave. For isotropic media, the one-way wave-equation operator does not change. For vertical transversely isotropic (VTI) media, one-way wave-equation operators for tilted transversely isotropic (TI) media are required because of the rotation of the coordinates. I apply this method to the BP 2004 velocity benchmark, to a synthetic dataset for VTI media, and to a real anisotropic dataset. The numerical examples show that plane-wave migration in tilted coordinates can image steeply dipping reflectors and overturned waves, and it is a good tool for salt delineation.

INTRODUCTION

Migration methods based on wave-equation extrapolation are gaining popularity in the industry. They can potentially better handle multi-pathing caused by complex geological structure. In nature, wave propagation has no directional preference: up-going and down-going waves propagate simultaneously. However, two-way wave-equation-based methods, such as reverse time migration (Whitmore, 1983; Baysal et al., 1983; Biondi and Shan, 2002), are still too expensive for today's computing resources. As a result, downward continuation (Claerbout, 1985), based on the one-way wave equation, is usually used. In downward-continuation methods, only down-going waves are allowed in the source wavefield, and only up-going waves are allowed in the receiver wavefield. Overturned waves, which travel downward first and then upward, are totally eliminated by the one-way wave equation. Even for waves only propagating upward or downward, it is difficult for downward-continuation methods to handle waves propagating far from the vertical direction in laterally varying media. As a result, downward-continuation methods have difficulty imaging steeply dipping reflectors.

A lot of effort has been made to improve the accuracy of one-way wave equation extrapolators in laterally varying media (Lee and Suh, 1985; Ristow and Ruhl, 1994; de Hoop, 1996; Huang and Wu, 1996). At the same time, people also design coordinates to make the extrapolation direction close to the propagation direction of waves, thereby reducing the accuracy

requirement of the extrapolator. These include tilted coordinates (Higginbotham et al., 1985; Etgen, 2002), beam migration (Brandsberg-Dahl and Etgen, 2003), and Riemannian coordinates (Sava and Fomel, 2005).

In this paper, we review plane-wave migration in tilted coordinates (Shan and Biondi, 2004). We present plane-wave migration in tilted coordinates for both isotropic and anisotropic media. Isotropic media are still isotropic after rotating the coordinates, while VTI media change to tilted TI media after rotating the coordinates. We use the one-way wave-equation extrapolation operator for tilted TI media proposed by Shan and Biondi (2005). We apply plane-wave migration in tilted coordinates to the BP synthetic velocity benchmark dataset (Billette and Brandsberg-Dahl, 2005), a synthetic dataset for VTI media, and an anisotropic real dataset.

PLANE-WAVE MIGRATION IN TILTED COORDINATES

Plane-wave (source plane-wave) migration (Whitmore, 1995; Rietveld, 1995; Duquet et al., 2001; Liu et al., 2002; Zhang et al., 2005) synthesizes plane-wave source experiments from shot records. The recorded data are decomposed into plane source gathers by slant-stack processing:

$$u(x_r, z=0; p; \omega) = \int U(x_r, z=0; x_s; \omega) e^{i\omega p x_s} dx_s, \tag{1}$$

where x_s is the source location, x_r is the receiver location, p is the ray parameter, U is the recorded surface data, and u is the synthesized surface data for the plane-wave source. The corresponding plane-source is

$$d(x_r, z=0; p; \omega) = e^{i\omega p x_s}. \tag{2}$$

The plane-wave source d and its corresponding synthesized data u are independently extrapolated into the subsurface, and the image can be obtained by cross-correlating these two wavefields. Plane-wave migration is potentially more efficient than shot-profile migration. It uses the whole seismic survey as the migration aperture, which is helpful for imaging steeply dipping reflectors.

Given the plane-wave source with a ray-parameter p, its take-off angle at the surface is $\arcsin(pv)$, where v is the surface velocity. we use tilted coordinates (x', z') satisfying

$$\begin{pmatrix} x' \\ z' \end{pmatrix} = \begin{pmatrix} \cos(\theta) & \sin(\theta) \\ -\sin(\theta) & \cos(\theta) \end{pmatrix} \begin{pmatrix} x \\ z \end{pmatrix}, \tag{3}$$

where (x, z) are Cartesian coordinates and θ is an angle close to the take-off angle of the plane-wave source at the surface. In the tilted coordinates, the extrapolation direction is potentially closer to the propagation direction. Therefore, in tilted coordinates, we can extrapolate the wavefield accurately with a less accurate extrapolator. Waves that were overturned in Cartesian coordinates are not overturned in tilted coordinates. Therefore, we can image them with the one-way wave equation.

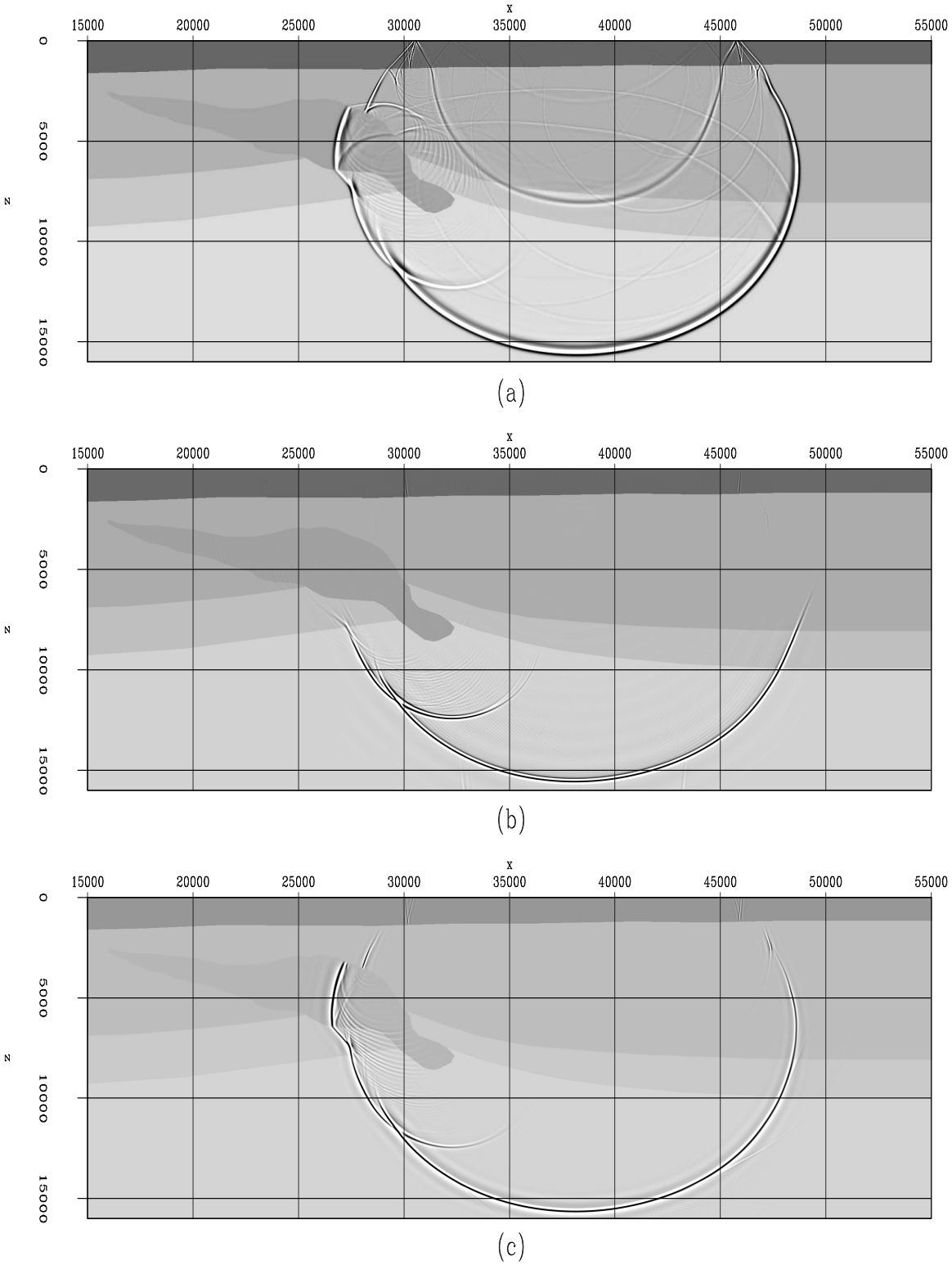

Figure 1: Impulse response of two-way wave equation (a), downward continuation (b), and the plane-wave migration in tilted coordinates (c). guojian1-impulse [CR]

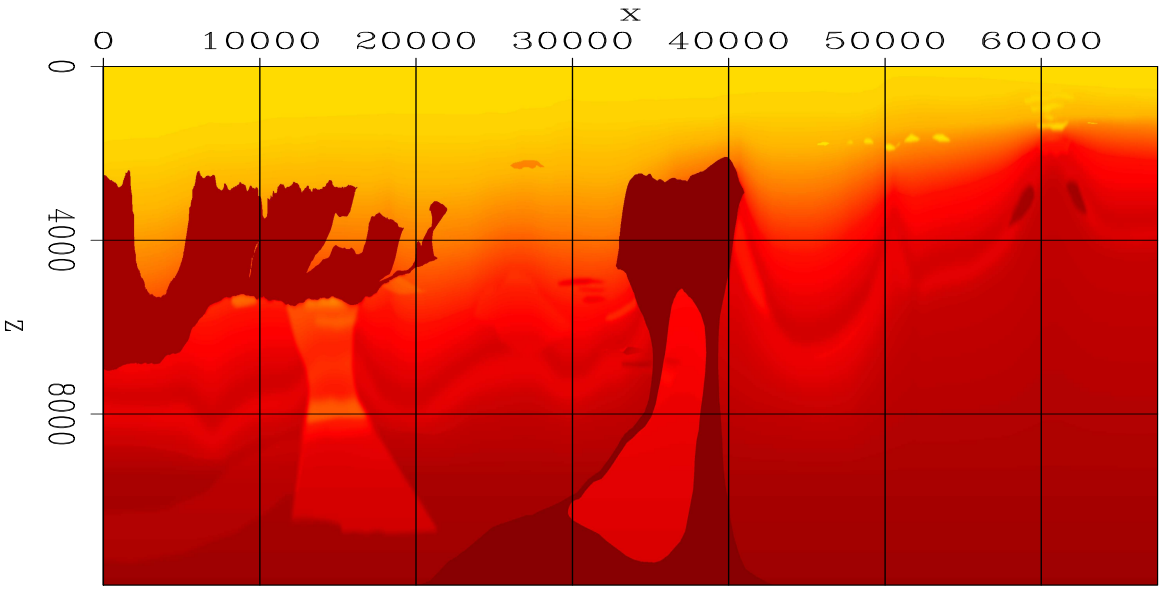

Figure 2: The velocity model. guojian1-bpvelall [ER]

NUMERICAL EXAMPLES

Impulse responses

Figure 1 compares the impulse responses of the two-way wave equation, the downward continuation and plane-wave migration in tilted coordinates. Figure 1(a) is the impulse response of the two-way wave equation, Figure 1(b) is the impulse response of downward continuation, and Figure 1(c) is the impulse response of plane-wave migration in tilted coordinates. In Figure 1(b), the small angle part of the wavefront is similar to that of the two-way wave equation, while the high angle part of the wavefront loses energy due to the overturned waves. In Figure 1(c), there are no reflections or multiples, since we still use the one-way wave-equation extrapolator, but the wave front of the direct arrival mimics that of the two-way wave equation very well, even at the high angle and with overturned waves.

BP 2004 velocity benchmark dataset

The BP synthetic dataset is designed to test velocity estimation. Figure 2 shows the velocity model of the dataset. One of the challenges for velocity analysis of this dataset is the delineation of the two salt bodies. The left one is a complex, multi-valued salt body with a greatly rugose top. Some parts of its top and flank and the sediments inside the salt are steeply dipping. These features are not easily imaged by downward continuation. The right salt body is deeply rooted, and its roots are very steep. Waves reflected at the center part of the two roots overturn and travel through the complex salt body to the left. Downward continuation loses the energy and cannot connect these two roots. Even with the true velocity, it is still chal-

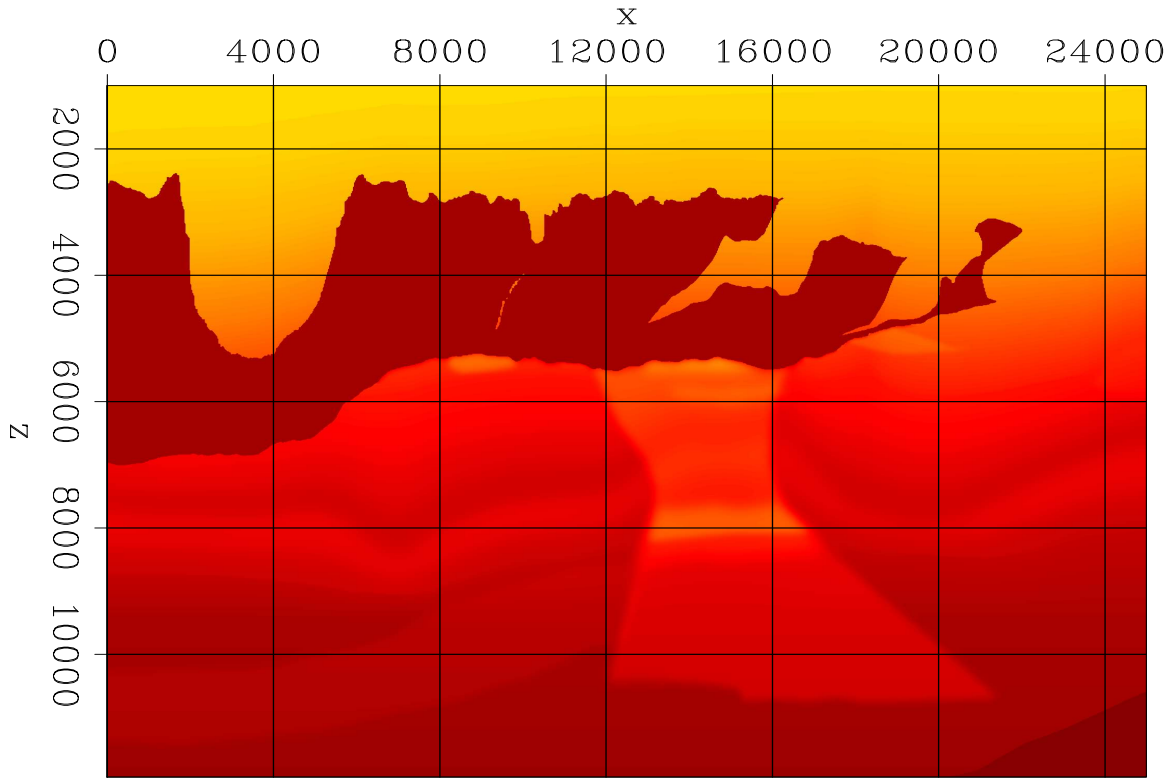

Figure 3: The velocity model of the left salt body. guojian1-bpvelleft [ER]

lenging to image the complex salt bodies. We run plane-wave migration in both Cartesian and tilted coordinates. We generate 200 plane-wave sources in total, and the take-off angles at the surface range from $-45°$ to $45°$. Since we do not run multiple attenuation, the images are contaminated by the multiples.

Figure 3 shows the velocity model of the left rugose salt body. Figures 4 and 5 show the images. Figure 4 is obtained by downward continuation, and Figure 5 is obtained by plane-wave migration in tilted coordinates. In Figure 4, the image of the top of the salt is not continuous. Some parts of the top are almost vertical and are lost in the downward continuation. This image captures only the bottom of the two canyons, and loses their flanks. Downward continuation also loses the steep salt flanks in the multi-valued area. These losses make picking the salt difficult. In contrast, plane-wave migration in tilted coordinates images the salt body very well and makes salt picking easier.

Figure 6 shows the velocity model of the right salt body. Figures 7 and 8 show the images. Figure 7 is obtained by downward continuation, and Figure 8 is obtained by plane-wave migration in tilted coordinates. Downward continuation loses the flanks of the top part of the salt. Due to overturned waves, downward continuation also loses the right leg and the center part of the left leg. In contrast, plane-wave migration images most parts of the salt flanks and the two legs. Hence, it is much easier to interpret the salt body from Figure 8.

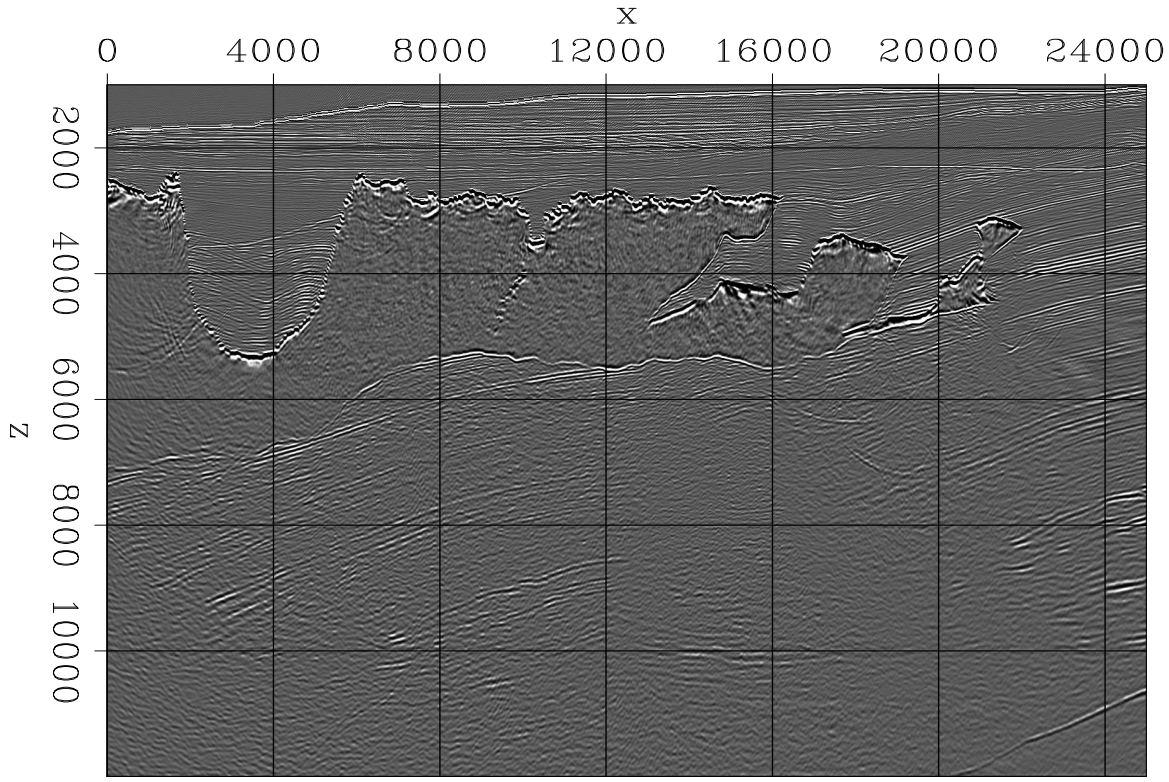

Figure 4: The image of the left salt body in Cartesian coordinates. guojian1-bpleftnotilt [CR]

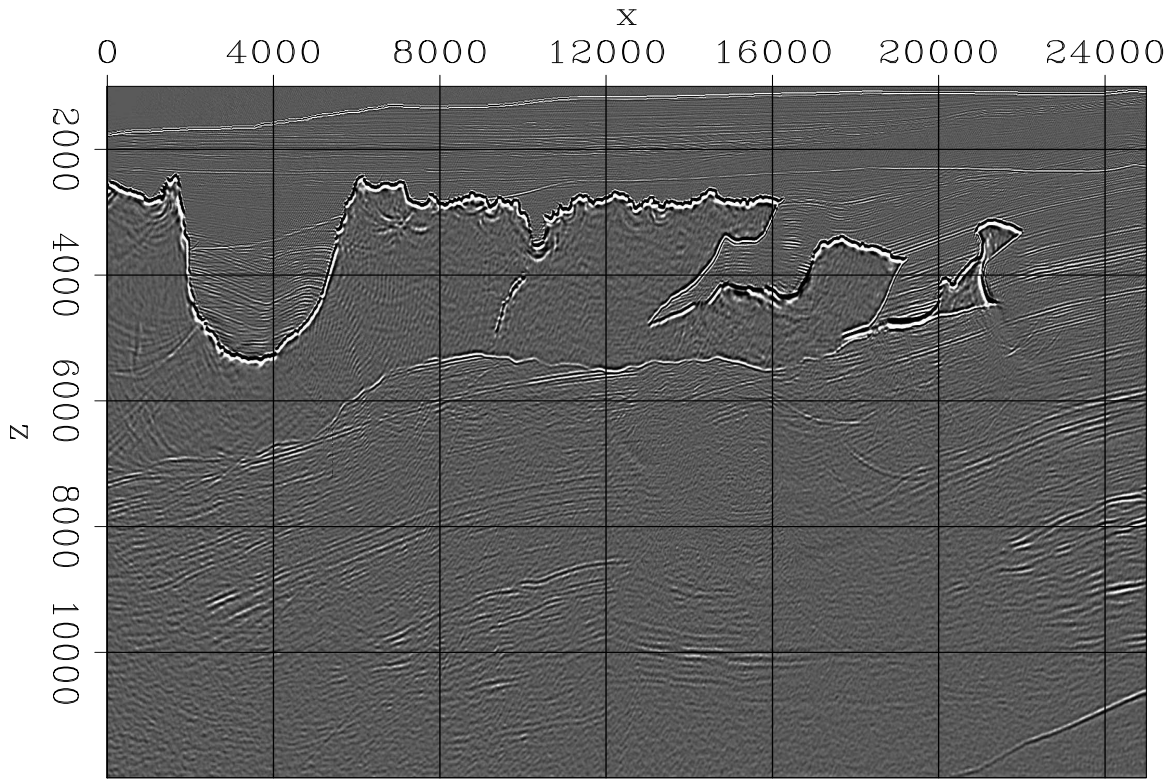

Figure 5: The image of the left salt body in tilted coordinates. guojian1-bplefttilt [CR]

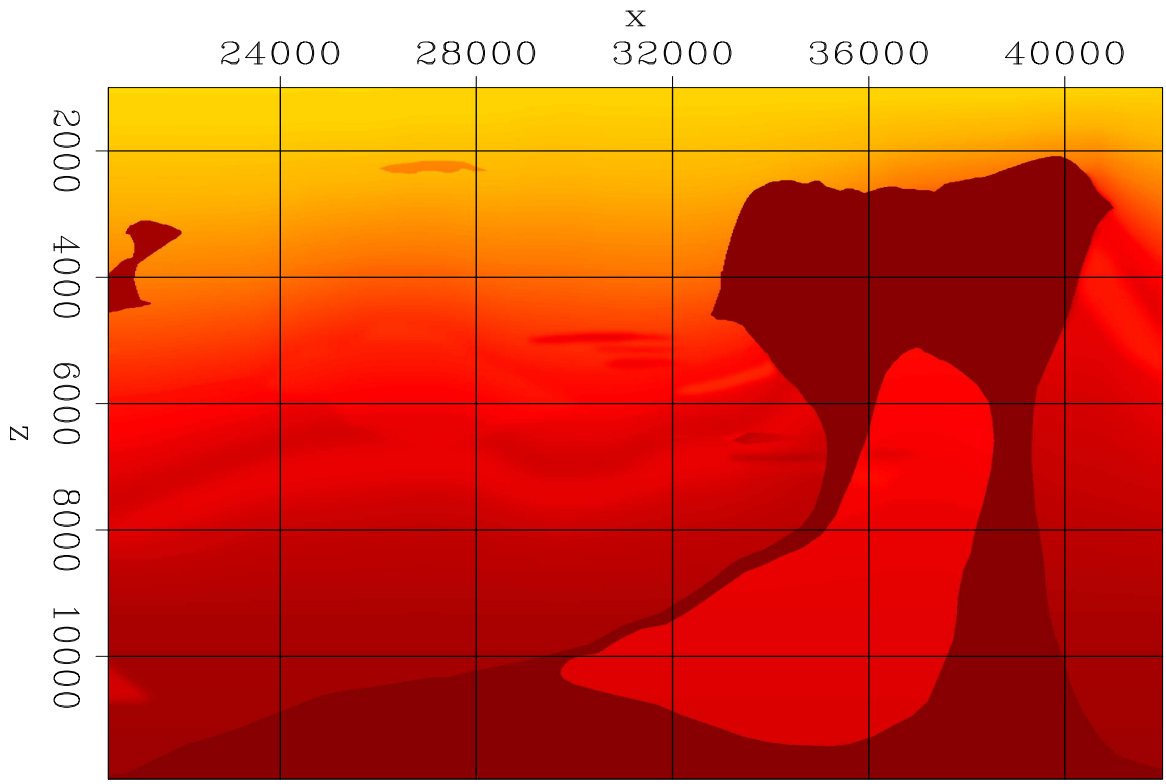

Figure 6: The velocity model of the right salt body. guojian1-bpvelright [ER]

A synthetic dataset for VTI media

Figures 9 – 11 show a synthetic model for a VTI medium. Figure 9 shows the velocity model, Figure 10 is the anisotropy parameter ε, and Figure 11 is the anisotropy parameter δ. There are 720 shots in total, and the maximum offset for each shot is 8000 meters. The challenging part of this model is to accurately image the steep fault, salt flank and the two abnormal sediments near the right corner of the salt body. I run plane-wave migration, using the extrapolation operator suggested by Shan and Biondi (2005). I generate 80 plane-wave sources, and the take-off angles at the surface range from $-40°$ to $40°$.

Figure 12 is the image obtained by isotropic plane-wave migration in tilted coordinates. Though we can see the energy of steeply dipping reflectors like the salt flanks and fault, they are not at the correct positions. Figure 13 is the image obtained by anisotropic plane-wave migration in Cartesian coordinates. The reflectors are at the right positions, but some parts of the steeply dipping salt flank are lost, and the bottom of the fault is not well focused. Also the bottom abnormal sediment at the right corner of the salt body loses its energy where it is close to the salt. Figure 14 is the image obtained by anisotropic plane-wave migration in tilted coordinates. In Figure 14, the salt flanks, the fault and abnormal sediments are all well imaged. Figure 15 overlays the image by anisotropic plane-wave migration in tilted coordinates with the actual model, and shows that the reflectors are imaged at the correction positions.

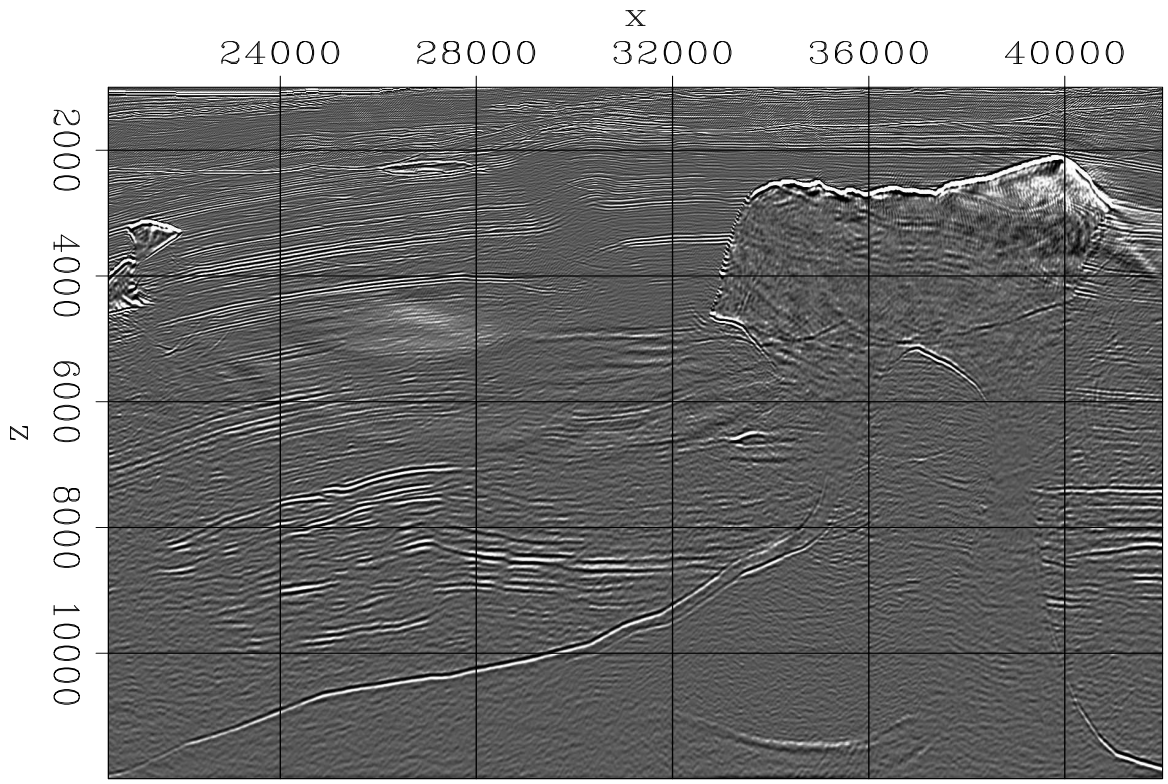

Figure 7: The image of the right salt body in Cartesian coordinates. guojian1-bprightnotilt [CR]

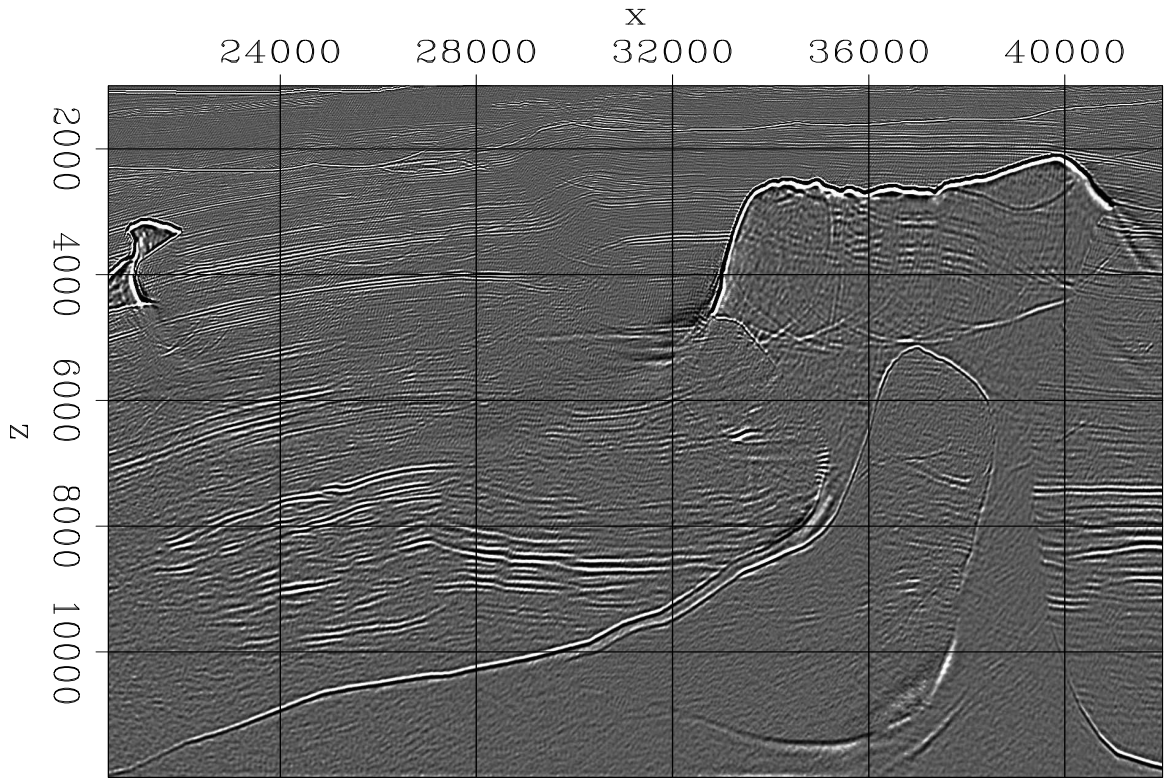

Figure 8: The image of the right salt body in tilted coordinates. guojian1-bprighttilt [CR]

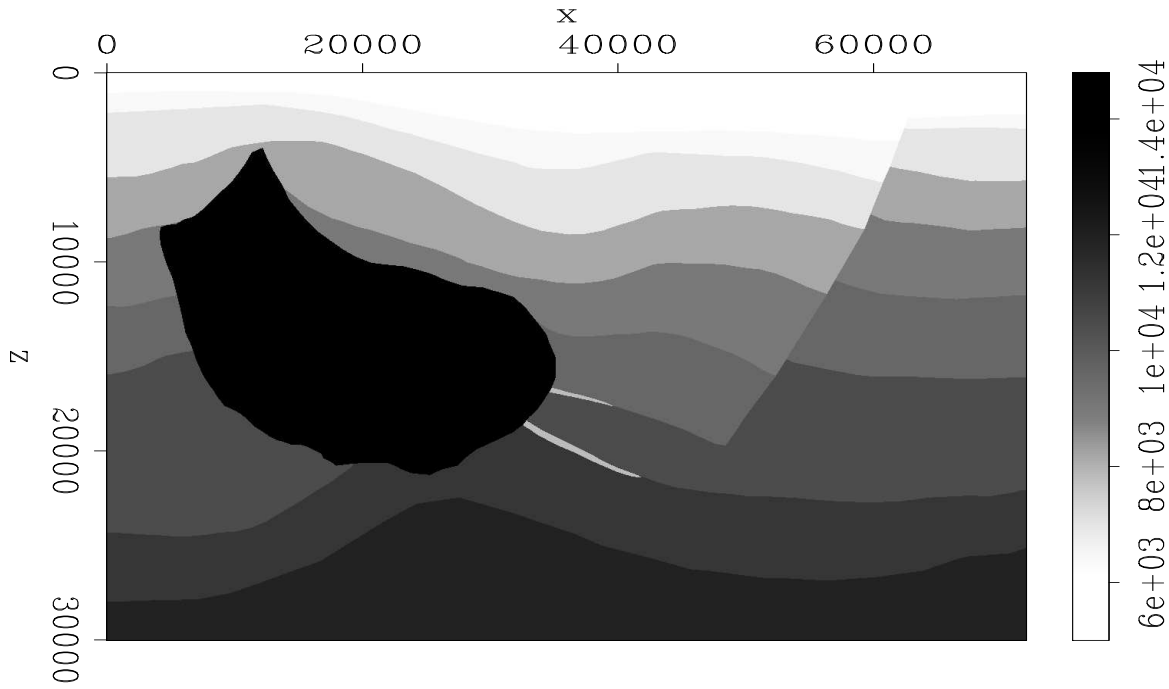

Figure 9: The vertical velocity model. guojian1-vpani [ER]

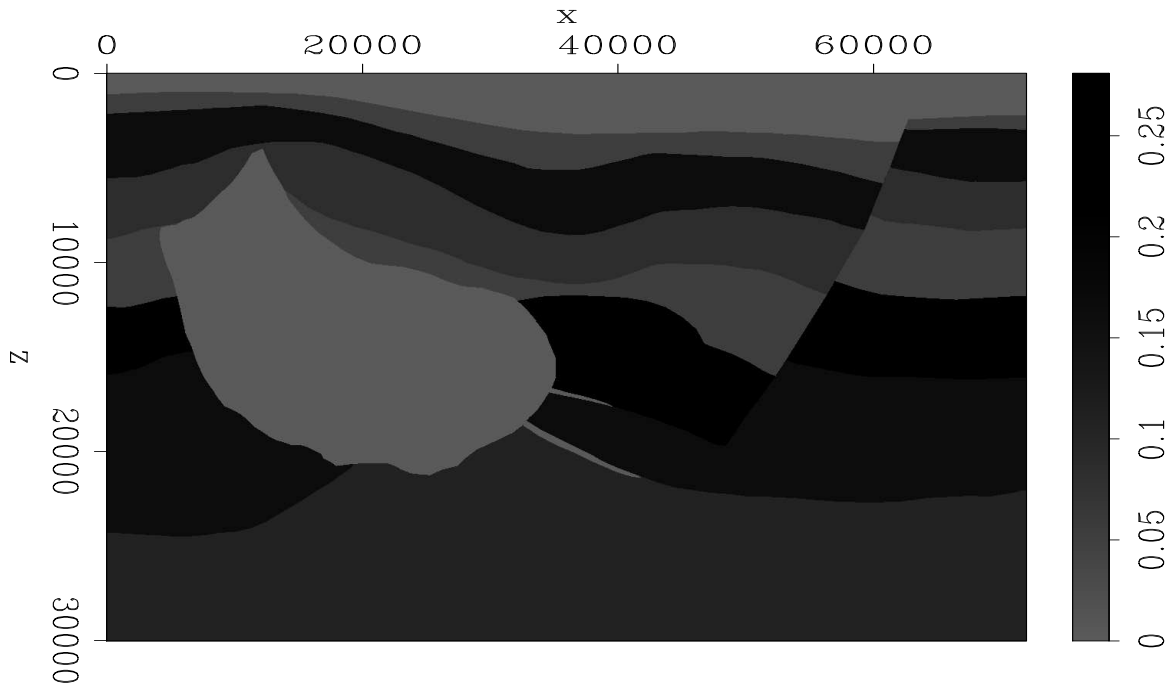

Figure 10: The anisotropy parameter ε. guojian1-epsani [ER]

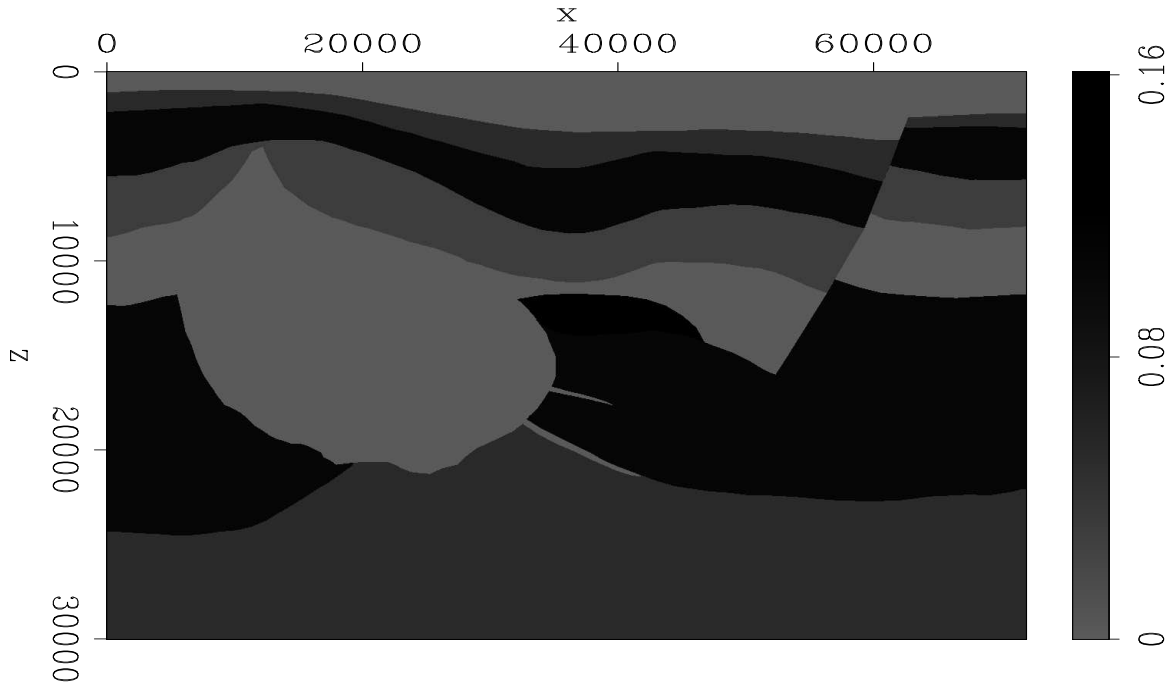

Figure 11: The anisotropy parameter δ. guojian1-dltani [ER]

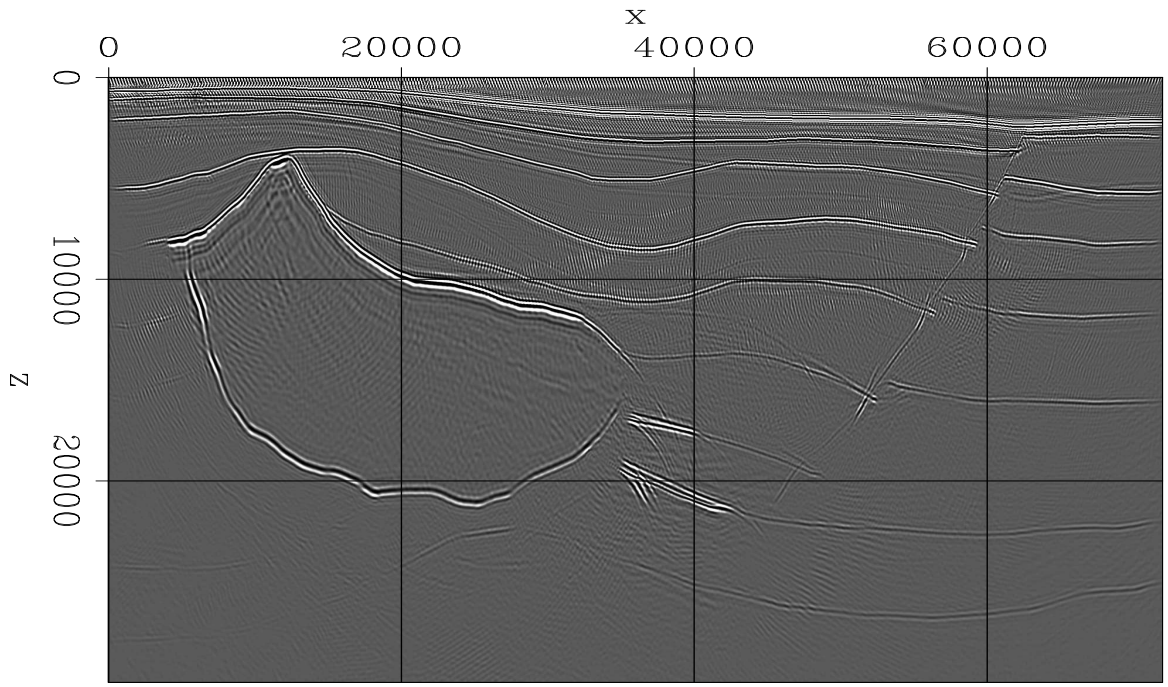

Figure 12: Isotropic migration in tilted coordinates. guojian1-isohesstilt [CR]

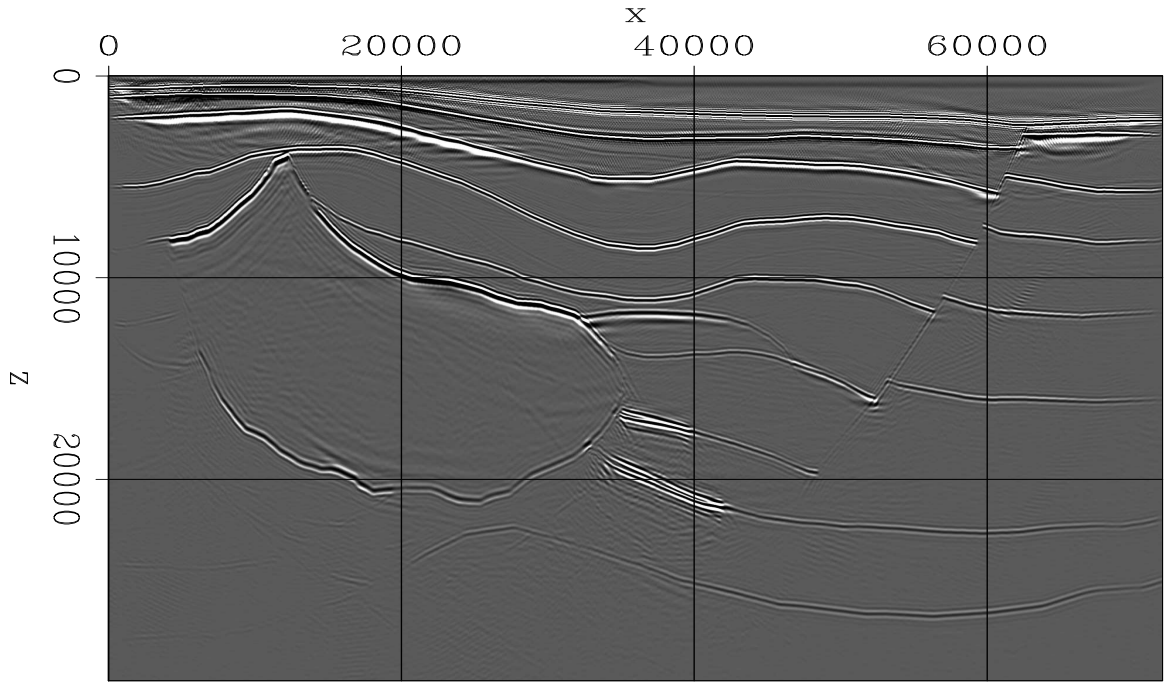

Figure 13: Anisotropic migration in Cartesian coordinates. guojian1-anihessnotilt [CR]

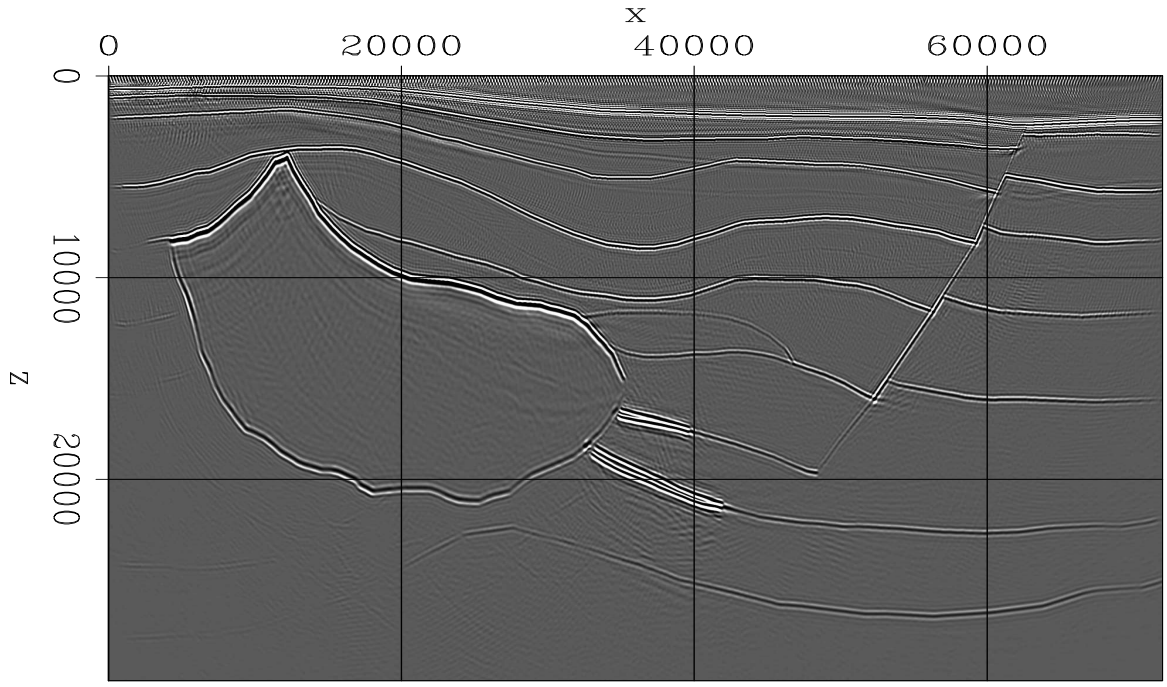

Figure 14: Anisotropic migration in tilted coordinates. guojian1-anihesstilt [CR]

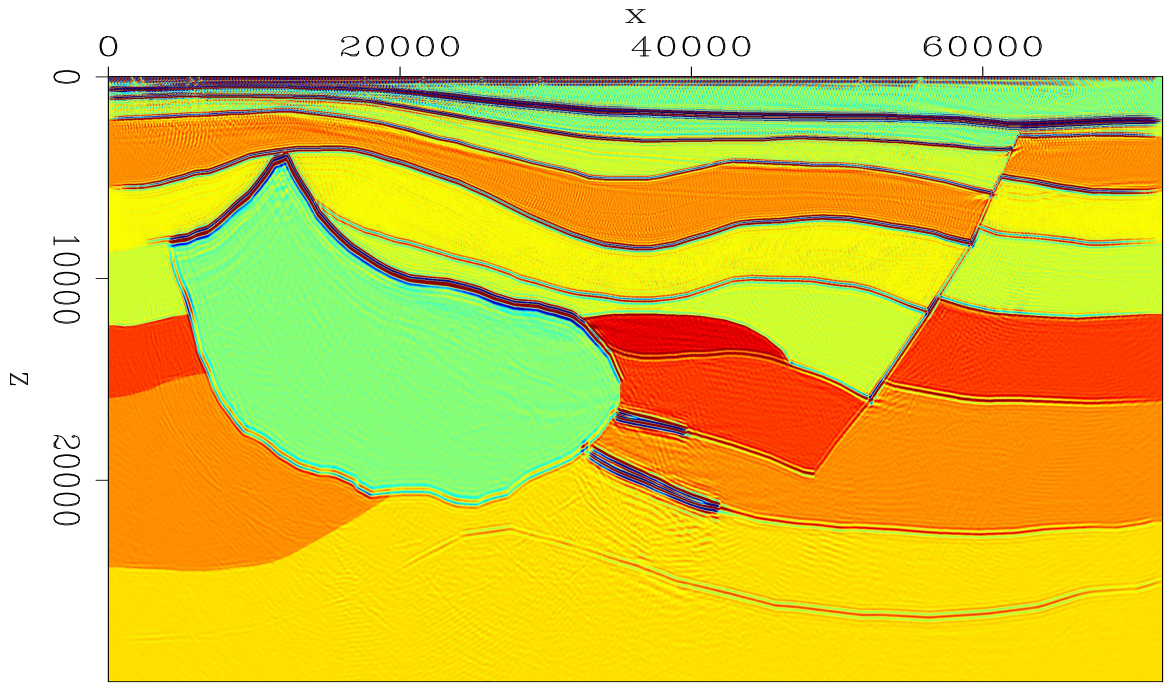

Figure 15: Anisotropic migration in tilted coordinates overlaid with the model. guojian1-anihesstilteps [CR]

A 2D slice of a real dataset from the Gulf of Mexico

In this 2D slice, there are 1600 shots, and the maximum offset is 4000 meters. I run plane-wave migration, using the wavefield-extrapolation operator suggested by Shan and Biondi (2005). I generate 80 plane-wave sources, for which the take-off angles at the surface range from -40° to 40°. Figure 16 is the image obtained by anisotropic plane-wave migration in Cartesian coordinates, and Figure 17 is the image obtained by anisotropic plane-wave migration in tilted coordinates. Figure 17 images the salt flank much better than Figure 16, and we can see a lot of small, steeply dipping events inside the shallow sediments that are quite continuous right to the edge of the salt.

CONCLUSION

We applied plane-wave migration in tilted coordinates on isotropic and anisotropic data. Plane-wave migration in tilted coordinates is potentially cheaper than shot-profile migration. For both isotropic and anisotropic data, plane-wave migration in tilted coordinates can handle overturned waves and image steeply dipping salt flanks and faults. It also images the rugose top of the salt very well. Plane-wave migration is a good tool for complex salt-body delineation.

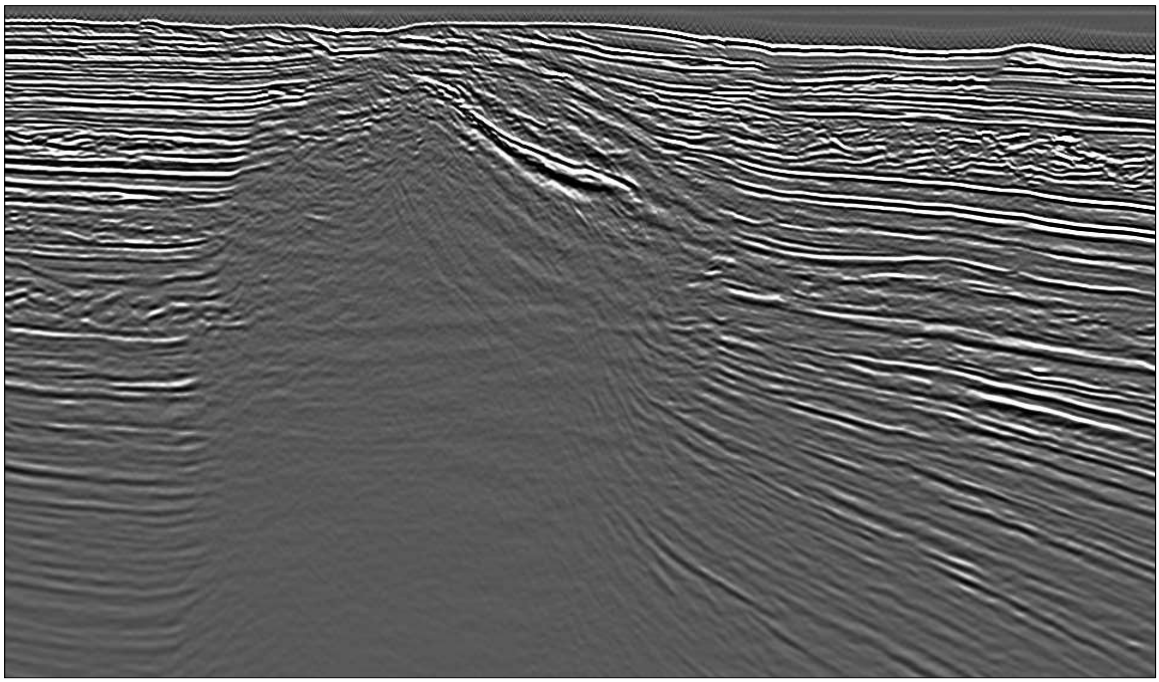

Figure 16: Anisotropic plane-wave migration in Cartesian coordinates. guojian1-aniexxonnotilt [CR]

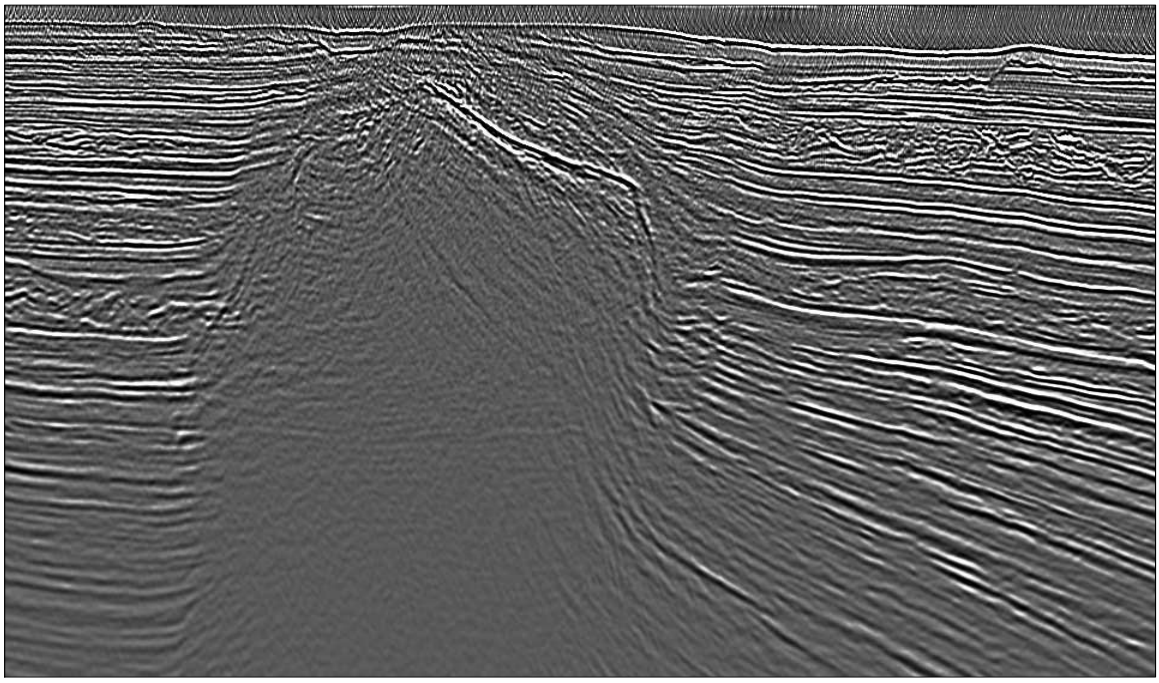

Figure 17: Anisotropic plane-wave migration in Cartesian coordinates. guojian1-aniexxontilt [CR]

ACKNOWLEDGMENTS

We thank Amerada Hess, BP, and ExxonMobil for making the data available. Guojian Shan also thanks Amerada Hess for the summer internship working on the synthetic data for VTI media.

REFERENCES

Baysal, E., Kosloff, D. D., and Sherwood, J. W. C., 1983, Reverse time migration: Geophysics, **48**, 1514–1524.

Billette, F., and Brandsberg-Dahl, S., 2005, The 2004 BP velocity benchmark: 67th meeting, Eur. Assn. Geosci. Eng., B035.

Biondi, B., and Shan, G., 2002, Prestack imaging of overturned reflections by reverse time migration *in* 72nd Ann. Internat. Mtg. Soc. of Expl. Geophys., 1284–1287.

Brandsberg-Dahl, S., and Etgen, J., 2003, Beam-wave imaging *in* Expanded Abstracts. Soc. of Expl. Geophys., 977–980.

Claerbout, J. F., 1985, Imaging the Earth's Interior: Blackwell Scientific Publications.

Duquet, B., Lailly, P., and Ehinger, A., 2001, 3-D plane wave migration of streamer data *in* 71st Ann. Internat. Mtg. Soc. of Expl. Geophys., 1033–1036.

Etgen, J., 2002, Waves, beams and dimensions: an illuminating if incoherent view of the future of migration: 72nd Ann. Internat. Mtg, Soc. of Expl. Geophys., invited presentation.

Higginbotham, J. H., Shin, Y., and Sukup, D. V., 1985, Directional depth migration (short note): Geophysics, **50**, 1784–1796.

de Hoop, M. V., 1996, Generalization of the Bremmer coupling series *in* J. Math. Phys. 3246–3282.

Huang, L. Y., and Wu, R. S., 1996, Prestack depth migration with acoustic screen propagators *in* 66th Ann. Internat. Mtg. Soc. of Expl. Geophys., 415–418.

Lee, M. W., and Suh, S. Y., 1985, Optimization of one-way wave-equations (short note): Geophysics, **50**, 1634–1637.

Liu, F., Stolt, R., Hanson, D., and Day, R., 2002, Plane wave source composition: An accurate phase encoding scheme for prestack migration *in* 72nd Ann. Internat. Mtg. Soc. of Expl. Geophys., 1156–1159.

Rietveld, W. E. A., 1995, Controlled illumination of prestack seismic migration *in* Ph.D. thesis. Delft University of Technology.

Ristow, D., and Ruhl, T., 1994, Fourier finite-difference migration: Geophysics, **59**, 1882–1893.

Sava, P., and Fomel, S., 2005, Riemannian wavefield extrapolation: Geophysics, **70**, T45–T56.

Shan, G., and Biondi, B., 2004, Imaging overturned waves by plane-wave migration in tilted coordinates: 74th Ann. Internat. Mtg., Soc. of Expl. Geophys., Expanded Abstracts, 969–972.

—, 2005, 3D wavefield extrapolation in laterally-varying tilted TI media: 75th Ann. Internat. Mtg., Soc. of Expl. Geophys., Expanded Abstracts, 104–107.

Whitmore, N. D., 1983, Iterative depth migration by backward time propagation *in* 53rd Ann. Internat. Mtg. Soc. of Expl. Geophys., Session:S10.1.

—, 1995, An imaging hierarchy for common angle plane wave seismograms *in* Ph.D. thesis. University of Tulsa.

Zhang, Y., Sun, J., Notfors, C., Gray, S., Chernis, L., and Young, J., 2005, Delayed-shot 3D depth migration: Geophysics, **70**, E21–E28.